



N63-13722
code-1

TECHNICAL NOTE

D-1717

ENERGY SPECTRUM OF ELECTRONS IN THE OUTER RADIATION BELT

Wilmot N. Hess and John A. Poirier

Goddard Space Flight Center
Greenbelt, Maryland

NATIONAL AERONAUTICS AND SPACE ADMINISTRATION
WASHINGTON

March 1963

891

Code - 1

SINGLE COPY ONLY

ENERGY SPECTRUM OF ELECTRONS IN THE OUTER RADIATION BELT

by

Wilmot N. Hess and John A. Poirier
Goddard Space Flight Center

SUMMARY

13722

The equilibrium energy spectrum of electrons in the outer radiation belt is determined by the injection spectrum and the loss processes that operate to remove the electrons or change their energy. The loss processes considered here are ionization energy loss, multiple scattering, and electron-electron scattering; the injection spectra considered are neutron β -decay electrons and monoenergetic electrons of 780 and 20 keV. The problem is treated numerically. The results of the numerical calculation are compared with recent measurements of the outer-belt electron spectrum; it appears that neutron decays produce a reasonable fraction of the outer-belt electrons, but other processes such as acceleration may be important.

CONTENTS

Summary	i
INTRODUCTION.	1
NUMERICAL CALCULATIONS.	4
RESULTS	6
The 780-kev Electron Problem	6
Neutron β -Decay Electrons	8
CONCLUSIONS.	11
ACKNOWLEDGMENTS	13
References	13

ENERGY SPECTRUM OF ELECTRONS IN THE OUTER RADIATION BELT *

by

Wilmot N. Hess and John A. Poirier†
Goddard Space Flight Center

INTRODUCTION

The sources of particles that populate the Van Allen radiation belts present an interesting problem. It is quite well established now that most of the protons in the inner belt come from the decay of neutrons leaking out of the earth's atmosphere (References 1 and 2). The source of electrons is not so well determined. It would be surprising if the electrons in the inner radiation belt were not also from leakage neutron decay (Reference 3), but this is not certain.

We will examine here the kind of an electron belt that would be produced at 2 or 3 earth radii out from the surface of the earth by neutron decay alone. We have detailed quantitative knowledge of the neutron-decay source strength (Reference 4) and therefore can quantitatively study the equilibrium electron spectrum to be expected in this region. Then, by comparison with experimental information about the outer radiation belt, we can see whether neutrons produce an important fraction of the outer belt.

We know the neutron source strength adequately but, to determine the equilibrium electron spectrum, we must understand the loss mechanisms operating to remove electrons. One such process is multiple small-angle Coulomb scattering (References 5, 6, and 7), which changes the pitch angle of the particles and lowers the mirror point so that the particles get lost in the atmosphere. Another process is ionization energy loss, which degrades the electron's energy. The former is proportional to Z^2 , where Z is the atomic number of the gas present; the latter is proportional to Z . Therefore the dominant loss mechanism depends on the type of material present.

Particles in the inner radiation belt move most of the time in an atmosphere of oxygen and nitrogen. The higher Z of this material is such that multiple scattering is the principal loss mechanism. Particles in the outer belt exist essentially in a hydrogen exosphere, where ionization energy loss is important.

*Also published in: *J. Geophys. Res.* 67(5):1699-1709, May 1962.

†Lawrence Radiation Laboratory, Univ. of California, Berkeley, California.

A typical high-energy electron in the outer radiation belt might move on a magnetic line of force going out 24,200 km from the center of the earth at the equator. Let us consider a 780-kev electron that has a mirror point at 30 degrees magnetic latitude. Let λ be the magnetic latitude of a field line, R the distance from the center of the earth, and α the pitch angle of the electron spiraling about the magnetic field line. $\tan \alpha = v_{\perp}/v_{\parallel}$, where v_{\perp} and v_{\parallel} are velocity components perpendicular and parallel to the magnetic field line respectively. Let us approximate the earth's magnetic field by a dipole field for which the field lines are given by

$$R = R_0 \cos^2 \lambda, \quad (1)$$

where R_0 is the radius of the field line at the equator ($\lambda = 0$). Its strength is given by

$$B = CR^{-3} \sqrt{1 + 3 \sin^2 \lambda}, \quad (2)$$

where $C = 8.1 \times 10^{10}$ gauss-km³. The pitch angle of the electron must satisfy the relation

$$B = B_m \sin^2 \alpha, \quad (3)$$

where B_m is the value of the magnetic field at the mirror point. Table 1 gives values of α and λ that satisfy Equations 1, 2, and 3 for: (a) a mirror point at 17,200 km, and (b) a mirror point at 8000 km.

Table 1
Values of α and λ Satisfying Equations 1, 2, and 3 for a Mirror Point
at (a) 17,200 km and (b) 8000 km.

R (km)	λ (deg)	α (deg)	
		Case (a)	Case (b)
24,200	0	34.4	8.3
17,200	30	90	14.8
8,000	54.9	—	90

Essentially, to lose a particle from the radiation belt by scattering, its angle must be altered so that the mirror point is lowered to about 8000 km, where it will encounter a relatively dense atmosphere. Table 1 shows that, if the scattering takes place at the equator, a change of pitch angle of 26.1 degrees is necessary to change the mirror point from 17,200 to 8000 km and, if the scattering takes place at 17,200 km, a change of 75.2 degrees is necessary. As an average intermediate situation, we will consider that a change of pitch angle of 1 radian will remove a particle from the outer belt. This corresponds to a scattering through a projected scattering angle of 1 radian, or a total scattering angle of $\sqrt{2}$ radians.

To determine which loss mechanisms are dominant in the outer belt, we must consider a change of pitch angle by Coulomb scattering and energy loss by ionization. For particles traveling in un-ionized hydrogen gas, Table 2 lists the probabilities of multiple scattering and single scattering to projected angles greater than 1 radian, and scattering from an electron that produces a recoil electron of greater than 30 kev energy. This calculation is summarized in Table 2 as a function of the particle's range.

Table 2
Summary of Scattering Probabilities as a Function of Particle Range.

E (kev)	R (gm/cm ²)	ΔR (gm/cm ²)	\bar{E} (kev)	$\overline{\theta_p^2}$ (rad ²)	$\Sigma \overline{\theta_p^2}$ (rad ²)	ΣP_{MS}	ΣP_{SS}	ΣN_{ee}
780	0.153	0.020	740	0.016	0.016	0.0	0.0005	0.11
700	0.133	0.025	650	0.026	0.042	0.0	0.0012	0.24
600	0.108	0.024	550	0.033	0.075	0.0003	0.0023	0.37
500	0.084	0.023	450	0.045	0.12	0.0031	0.0037	0.50
400	0.061	0.0213	350	0.065	0.19	0.024	0.0059	0.63
300	0.0397	0.0187	250	0.10	0.29	0.064	0.0097	0.74
200	0.0210	0.0144	150	0.19	0.48	0.16	0.018	0.83
100	0.00657	0.00463	75	0.20	0.68	0.22	0.029	0.85
50	0.00194							

Here E is the electron kinetic energy in kev, R is its range in hydrogen in gm/cm² (Reference 8), ΔR is the amount of hydrogen necessary to lower the electron energy from the top to the bottom of the energy group indicated, \bar{E} is the average kinetic energy of the group in kev, $\overline{\theta_p^2}$ is the square of the rms projected multiple-scattering angle in rad² (Reference 9), $\Sigma \overline{\theta_p^2}$ is the sum of these angles to get the additive effect, ΣP_{MS} is the probability that this value of $\Sigma \overline{\theta_p^2}$ will scatter the particle downward 1 radian or more, ΣP_{SS} is the probability that the electron will single-scatter 1 radian or more in the projected angle downwards, and ΣN_{ee} is the number of recoil electrons from electron-electron collisions having energy 30 kev or higher (Reference 9).

Inspection of this table shows that an electron will slow down from 780 to about 50 kev before the scattering gets large enough that a significant number of particles will be lost from the outer belt ($\Sigma P_{MS} = 0.22$ at 50 kev). Below 50 kev, the scattering increases sharply, and a substantial fraction of the particles will be lost by scattering. Only about a quarter of the particles in the outer belt will scatter out of the belt when a 780-kev electron slows down to 50 kev. About one secondary electron of energy greater than 30 kev will be made per 780-kev electron slowing down. Thus in the numerical calculation to follow we must consider both slowing down and scattering as important loss mechanisms in the outer zone, with the additional production of low-energy electrons by electron-electron collisions.

NUMERICAL CALCULATIONS

The scattering calculations were coded for an IBM 709 computer. The program was run with several input spectra. The first problem was started by having all particles in one energy group (770 to 778 kev) and was stopped when all particles were slowed down below 30 kev. This case of a monoenergetic pulse source can be checked analytically, and it demonstrates the kinds of physical processes that take place. This problem is moderately similar to what happened in the Argus experiment when a pulse of electrons was suddenly injected into the earth's magnetic field by a nuclear explosion (Reference 10).

The second calculation starts with the neutron β -decay spectrum and follows these particles down to 30 kev. This problem has a bearing on the makeup of the outer radiation belt.

Each of these calculations have been studied for: (1) a pulse source, and (2) a continuous source. In case (1) a squirt of particles is started all at one time and slowed down together. In case (2) the same number of particles are injected at each interval in time, and the problem is carried forward until an equilibrium spectrum is obtained.

The computer program starts with an initial spectrum and calculates the spectrum after a short time Δt . The time step is taken short enough that the probability of a particle with $E = 30$ kev scattering twice in one time step is very small. The process is repeated for many time steps until the problem is completed. Three loss mechanisms have been considered: (a) the usual ionization energy loss for a moving charged particle having distant collisions with electrons (dE/dx); (b) close collisions with electrons, which occur less frequently but are important in that larger momentum transfers are involved and new, fast particles can be made in this way; and (c) the loss by scattering, which removes particles from the region by changing the pitch angle.

Loss processes (a) and (b) are handled together, while (c) is considered separately. To handle (c), we calculate how many particles $S(E)$ are lost from each energy group in each time step by scattering. The fraction of particles scattering in each step is obtained from

$$S(E) = \frac{\Delta t \bar{\rho}}{[\rho \tau(E)]} \quad (4)$$

where $\bar{\rho}$ is the number of protons per cubic centimeter traversed by the electron and $\bar{\rho} \tau(E)$ is the product of proton density and electron lifetime as calculated by Wentworth, MacDonald, and Singer (Reference 7).

The energy loss processes (a) and (b) have been represented by

$$\begin{aligned} N^i(m+1) = & N^i(m) + \sum_{l=i+1}^{l_{\max}} N^l(m) P_l^i - N^i(m) \sum_{l=i/2}^{i-1} P_l^i \\ & - N^i(m) \left| \frac{dE^i}{dx} \right|_c \frac{\Delta x^i}{\Delta E} + N^{i+1}(m) \left| \frac{dE^{i+1}}{dx} \right|_c \frac{\Delta x^{i+1}}{\Delta E} \end{aligned} \quad (5)$$

which relates the number of particles in the i^{th} energy group at time step $m + 1$, $N^i(m + 1)$, to those in that group at time step m , $N^i(m)$. Here P_i^l is the probability that an electron be scattered from group l (superscript) to group i (subscript) by an electron-electron scatter. The first term on the right side of Equation 5 is the number of particles in group i just before time step $m + 1$. The second term is the number that scatter into group i from energies above it; this electron may be a recoil electron or a higher energy electron that has been degraded in energy (these two electrons are indistinguishable). The third term is the number of particles that scatter out of group i into lower energy groups. The fourth term is the number of particles that lose enough energy by ionization to be degraded from the i^{th} group to the next lower energy group. The last term is the number of particles in the $i = 1$ group that lose enough energy to be degraded into the i^{th} group.

The probability P_i^l is

$$P_i^l = (\nu \rho_e \Delta t) \left(\frac{d\sigma_{ee}}{dW} \right) \Delta E^i, \quad (6)$$

where ρ_e is the electron density. In Equation 6 the electron-electron scattering cross section has been calculated by C. Møller (Reference 11):

$$\frac{d\sigma_{ee}}{dW} = \frac{2\pi r_0^2}{\beta^2} (mc^2) \left[\frac{1}{W^2} + \frac{1}{(E - W)^2} + \frac{1}{(E + mc^2)^2} - \frac{2E + mc^2}{(E + mc^2)^2} \frac{1}{W(E - W)} \right], \quad (7)$$

where $2\pi r_0^2 = 2\pi(e^2/mc^2)^2 = 0.50 \times 10^{-24} \text{ cm}^2$; $\beta = v/c$ for the incident electron; m is the rest-mass energy of the electron; E is the incident-electron kinetic energy; and W is the kinetic energy of either of the two final electrons. All quantities are expressed in the laboratory coordinate system.

The ordinary ionization energy loss corrected for that part of the energy loss that has already been included as large-angle scattering in the second and third terms in Equation 5 is

$$\left| \frac{dE^i}{dx} \right|_c = \left| \frac{dE^i}{dx} \right| - \sum_{l=i/2}^{i-1} \frac{d^2 P_l^i}{dE dx} (E^i - E^l) \Delta E, \quad (8)$$

where (Reference 12)

$$\left| \frac{dE}{dx} \right| = \rho_e mc^2 \frac{2\pi r_0^2}{\beta^2} \left[\log_e \frac{mc^2 E \beta^2}{2I^2 (1 - \beta^2)} - \left(2\sqrt{1 - \beta^2} - 1 + \beta^2 \right) \log_e 2 + 1 - \beta^2 + \frac{1}{8} (1 - \sqrt{1 - \beta^2})^2 \right]. \quad (9)$$

Here ρ_e is the number of electrons per cubic centimeter, I is the ionization energy constant, and the rest of the symbols are as defined above.

Combining Equations 5 and 8, we get

$$\begin{aligned}
N^i(m+1) = & N^i(m) + \sum_{l=i+1}^{l_{max}} N^l(m) P_l^i + N^i(m) \sum_{l=i/2}^{i-1} (i-l-1) P_l^i \\
& + N^{i+1}(m) \left| \frac{dE^{i+1}}{dx} \right| \frac{\beta^{i+1} c \Delta t}{\Delta E} - N^i(m) \left| \frac{dE^i}{dx} \right| \frac{\beta^i c \Delta t}{\Delta E} \\
& - N^{i+1}(m) \sum_{l=(i+1)/2}^{l_{max}} (i-l+1) P_l^{i+1} .
\end{aligned} \tag{10}$$

In the energy region from 30 to 60 Mev, additional approximations have improved the convergence of the sums. The character of the spectrum on either side of 60 kev lends validity to these approximations.

The calculation for each time step is repeated until all particles have slowed down below 30 kev. The time interval Δt has been selected to be small enough so that there is a very small chance that a particle will be scattered twice within that time step. Since the chance of scattering goes up with a decrease in particle energy, a compromise must be made between computer time and the lowest energy of interest. On this basis, the lowest energy of interest was chosen to be 30 kev.

RESULTS

As was stated before, in the first problem we started with a pulse of particles at $E = 780$ kev and followed them as they produced secondary electrons, were slowed down by ionization energy loss, and were scattered out. The starting datum of the second problem was the neutron-decay spectrum.

The 780-kev Electron Problem

The first problem was undertaken to demonstrate the physics in the slowing-down problem. Starting with all the particles at 780 kev, the calculation proceeds until all the particles slow down to less than 30 kev. Figure 1 shows several steps in the slowing-down process. In a short time, the initial pulse of particles, point A in Figure 1, turns into a U-shaped distribution, curve B, by producing knock-on electrons. Curves B, C, D, and E are drawn for equal time intervals where the energy loss by ionization as well as the buildup of low-energy recoil electrons can easily be seen. Curve C' (dashed line) is the solution for the problem ignoring the scattering-out term. We see that the effect of this scattering-out term becomes large only for energies below about 100 kev. Eventually all the particles are lost by scattering or pass below the energy cutoff of the problem. It should be pointed out that these figures give the density of particles at a given energy (electrons/cm³). If a flux of particles is desired (electrons/cm²-sec), the spectra must be multiplied by the appropriate velocity.

The Argus nuclear explosion (Reference 13), carried out at about 300 miles above the earth, formed a shell of trapped electrons in space. The electrons were produced by β -decay of the fission fragments from the explosion. These electrons were lost eventually by multiple small-angle Coulomb scattering (Reference 6) on the oxygen and nitrogen atoms in the atmosphere. However, if the Argus explosions had been at an altitude of 2000 km or more and had therefore been in the hydrogen exosphere, the electron spectrum would have behaved roughly as is shown in Figure 1 because of the three loss mechanisms considered. There is, of course, a spectrum of energy for electrons born of a nuclear explosion, some of which have energies of more than 1 Mev. The physical processes remain the same however, and the above solution for a δ -function input should give a qualitative feeling for what would be expected for a high-altitude Argus experiment.

If we consider a situation where a stream of 780-keV electrons is continuously introduced into the magnetic field, an equilibrium spectrum will result. The solid line A in Figure 2 shows the spectrum that would result after equilibrium is established. The total number of particles as a function of the time after initiating the injection (the buildup toward equilibrium) is given in Figure 3, curve B. An example of this physical process might be a particle accelerator in space continuously emitting a beam of 780-keV electrons (Reference 13).

Several checks have been made to insure that the computer program was doing the desired calculation. One such check has been indicated in Figure 2 by a dashed line, curve B. This line indicates the equilibrium spectra that would be attained if there were a continuous source of 780-keV electrons and the only loss mechanism was ionization energy loss. This

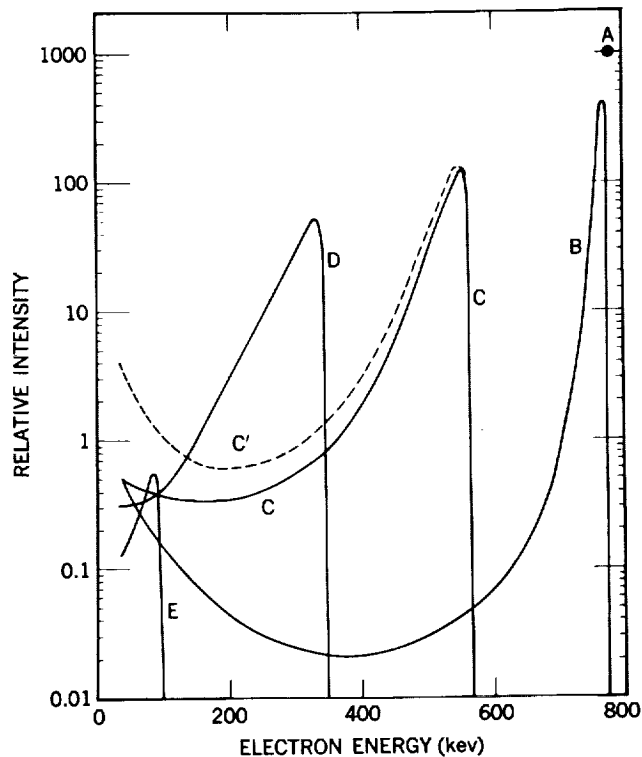


Figure 1—A single group of electrons injected at 780 keV (point A) are slowed down, produce knock-on electrons, and scatter out of the region of interest in the outer belt. Curve B shows a time soon after the injection time; curves C, D, and E are at equal time intervals after injection. The dotted part of curve C shows the effect of not including the Coulomb scattering-out term in the calculation.

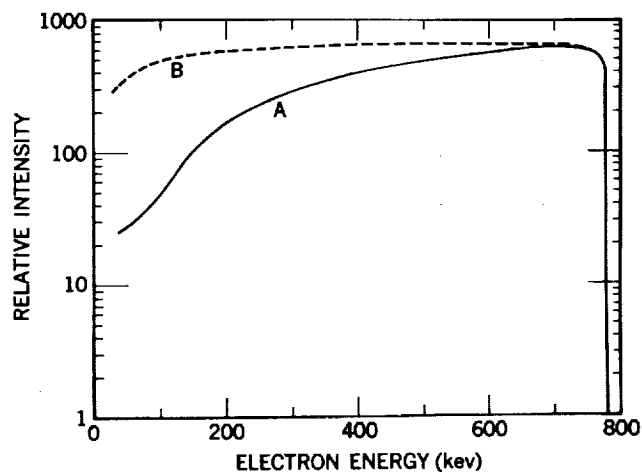


Figure 2—Curve A is the equilibrium spectrum produced by a continuous injection of electrons of 780-keV energy into the outer radiation belt. The dashed curve B is the equilibrium spectrum if we assume that ionization energy loss is the sole loss mechanism.

case can easily be calculated analytically, and the results agree with the machine calculations. To illustrate the nature of the analytic solution, first assume that dE/dx (ionization energy loss per centimeter of stopping material) has the simplified form

$$\frac{dE}{dx} \approx kv^{-2}, \quad (11)$$

where k is a constant and v the electron velocity. The probability dP/dE of finding a particle between energy E and dE is directly proportional to the time dt that the particle spends in this energy interval.

Therefore we can write

$$\frac{dP(E)}{dE} = \frac{dt}{dE} = \left[\frac{dE}{dx} \frac{dx}{dt} \right]^{-1} \approx \frac{v}{k} = \frac{1}{k} \frac{(E^2 + 2Em)^{1/2}}{E + m}, \quad (12)$$

where m is the mass and E the kinetic energy of the electron. Starting with the relativistic dE/dx formula, Equation 9, for the ionization energy loss of electrons, a correct relativistic calculation of dP/dE has been made following the above outline. Results of this analytic calculation agree very closely with those of the corresponding machine calculation, which is shown by curve B in Figure 2.

Neutron β -Decay Electrons

The main purpose of this paper is to calculate what electron spectrum would exist in the outer radiation belt resulting from neutron β -decay electrons alone. Starting with a pulse of neutron β -decay electrons (curve A, Figure 4), the calculations proceed as before. The slowing down and scattering out is shown in several stages in Figure 4. Curves B, C, and D are drawn for equal time intervals.

The equilibrium spectrum (curve A, Figure 5) is compared with the original β -decay spectra, curve B in Figure 5. Curve A in Figure 5 is the electron energy spectrum that would exist in the outer radiation belt if neutron decay was the only source of electrons and we had considered all the loss

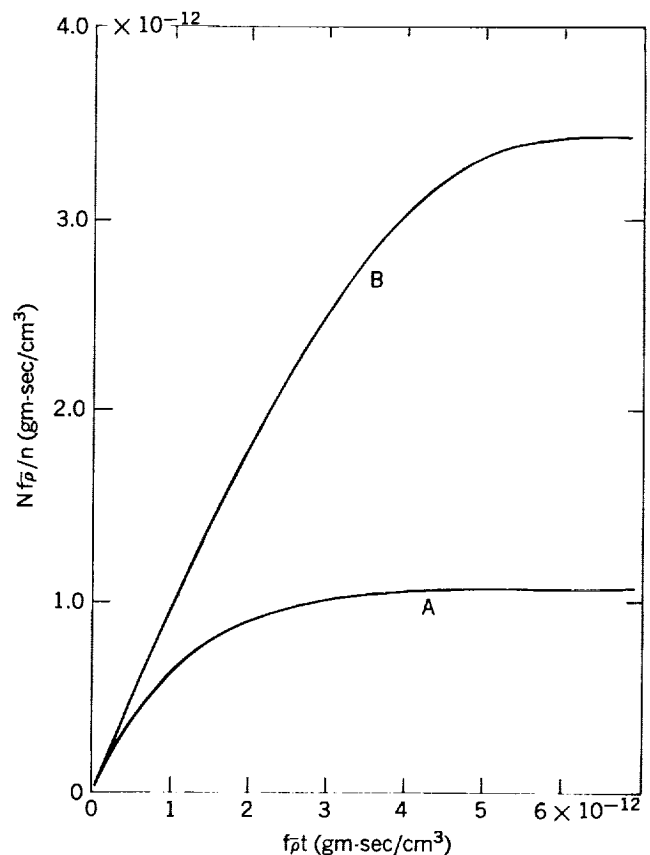


Figure 3—The buildup toward equilibrium by a continuous injection of electrons in the outer belt. Curve A is, in units defined below, the total number of electrons (above 30 kev) as a function of time after the start of uniform injection of electrons with a β -decay energy spectrum. Curve B is the same quantity for a δ -function source of electrons at 780-kev kinetic energy. On the abscissa the quantity $f\bar{\rho}t$ is plotted in gm-sec/cm³, where t is the time in seconds, $\bar{\rho}$ is the average density of hydrogen in gm/cm³, and f is a factor that describes the increased effectiveness of a partially ionized medium to multiple-scatter and absorb energy by ionization energy loss (see text). The quantity $Nf\bar{\rho}/n$ is plotted on the ordinate, where N is the number of electrons/cm³ at equilibrium and n is the number of electrons/cm³-sec that are injected.

processes. These data are also electron density rather than flux. We see that the equilibrium spectra is much the same shape as the original β -decay spectrum except for a slight shift toward lower energy. The buildup toward equilibrium as a function of time is shown in Figure 3, curve A. This figure gives the total number N of particles with energies greater than 30 kev as a function of time t . The units on the abscissa are $f\bar{\rho}t$, where f is a dimensionless number that characterizes the increased effectiveness of a partially ionized medium to multiple-scatter or to lose energy by ionization energy loss, $\bar{\rho}$ is the average density in gm/cm^3 , and t is the time in seconds. The units on the ordinate are $f\bar{\rho}N/n$, where N is the number of particles/ cm^3 in the radiation belt and n is the rate of injection in electrons/ $\text{cm}^3\text{-sec}$.

For example, assume that a particle mirrors at 30 degrees magnetic latitude on the line that reaches a maximum distance of 3.8 earth radii from the center of the earth. Assume that the hydrogen is 50 percent ionized and has an average density of $10^{-21} \text{ gm}/\text{cm}^3$ (References 14 and 15). From Figure 3 we see that the electron spectra reaches 50 percent of its equilibrium value for $f\bar{\rho}t = 0.8 \times 10^{-12} \text{ gm-sec}/\text{cm}^3$. Here f is

$$f = \frac{\left| \frac{dE}{dx} \right|_{\text{ion}} f_{\text{ion}} + \left| \frac{dE}{dx} \right|_{\text{neut}} f_{\text{neut}}}{\left| \frac{dE}{dx} \right|_{\text{neut}}} \quad (13)$$

where $|dE/dx|_{\text{ion}}$ is the ionization energy loss by completely ionized hydrogen and f_{ion} is the fraction of the hydrogen that is ionized. The subscript "neut" denotes the corresponding quantities for neutral hydrogen. The same kind of an equation can be written for the multiple-scattering angle (Reference 16). For any value of f_{ion} , f has values that range from 1 when

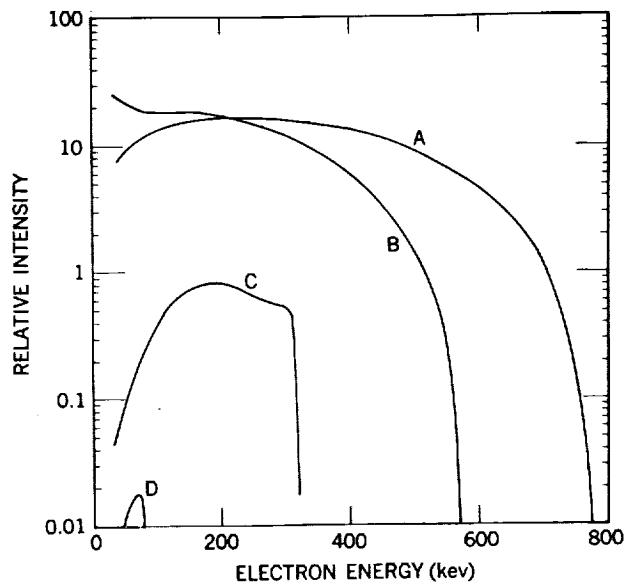


Figure 4—Curve A is the neutron β -decay energy spectrum. Curves B, C, and D show the changes that would occur at equal time intervals after a single burst of β -decay electrons.

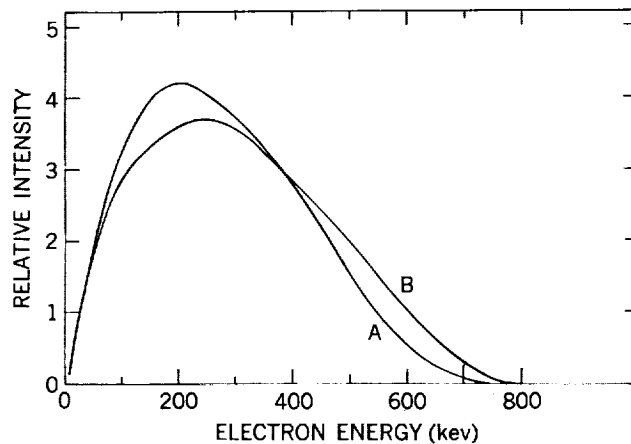


Figure 5—Curve B is the electron energy spectrum from neutron β decay. With this as the energy spectrum of the electrons injected into the outer belt, the equilibrium energy distribution of curve A was obtained after considering the loss processes discussed in the text. The plot is electron density (not flux) per kev on a linear scale.

$f_{ion} = 0$ to about 3 when $f_{ion} = 1.0$. If we assume $f = 2$, $\bar{\rho} = 10^{-21}$ gm/cm³, then the time for 50 per-cent equilibrium of neutron-decay electrons is 4×10^8 sec, or about 12 years. The equilibrium intensity may be obtained from $Nf\bar{\rho}/n = 10^{-12}$ gm-sec/cm³ (curve A, Figure 3). If we assume the electron injection rate $n = 3 \times 10^{-13}$ electrons/cm³-sec (Reference 4) and values of f and $\bar{\rho}$ as above, then $N = 1.5 \times 10^{-4}$ electrons/cm³. An approximate flux can be obtained by multiplying this figure by the most probable velocity of 2.2×10^{10} cm/sec, yielding a flux of 3.4×10^6 electrons/cm²-sec for neutron-decay electrons above 30-kev energy as a representative value for the outer belt. It should be noted that electron-electron scattering does not scale as above since it is independent of f at these energies. However this effect is not as large as that of ionization energy loss or multiple scattering, and f is bounded between 1.0 and 3.0. Therefore the scaling error should not be large. The numerical problem of this paper was performed with $f = 2.0$, and so it does not affect the example above. In Figure 3, then, f should not be a variable but should be set equal to 2.0.

The possibility has been suggested that there are a large number of low-energy electrons in the outer radiation belt (Reference 17). We have made a further calculation bearing on this low-energy group of electrons. A lifetime of about 1.5×10^7 sec is all that can be expected of a 20-kev electron in a hydrogen atmosphere of 1200 atoms/cm³ average density, because of its range and multiple-scattering loss. Thus 20-kev electrons must be injected at a rate of 7×10^{-7} electrons/cm³-sec to achieve equilibrium fluxes of 10^{11} electrons/cm²-sec. This source strength is about 10^7 times that of the neutron β -decay source.

The spectrum calculated here is for neutron β -decay electrons trapped in the outer Van Allen radiation belt. We would expect, however, that the spectrum at lower altitudes would be different, even on magnetic field lines that extend into the upper belt. We attempted to see how this spectrum at lower altitude would differ from that in the upper altitudes by keeping track of the number and energy of those electrons that were Coulomb-scattered out of the upper radiation belt. These particles are the ones whose mirror altitude is lowered, and therefore they feed the spectrum at lower altitudes. Using these scattered particles as an input spectrum for lower altitudes and using a lifetime proportional to E^2 for electrons in the nitrogen-oxygen atmosphere of lower altitudes (Reference 6), we obtain a flux spectrum as shown in Figure 6. It should be emphasized that the geometry used is not that of the radiation belts. Essentially, we have put electrons in a box of hydrogen and calculated the equilibrium spectrum inside the box. We also calculated the energy spectrum of particles scattered out of this box and weighted them with the lifetime they would experience in the lower atmosphere. Kellog (Reference 18) has also calculated this leakage spectrum using an input spectrum of neutron β decay (our scattered spectrum has many more lower energy particles) and a loss mechanism of ionization energy loss [the E^2 lifetime of Welch and Whitaker (Reference 6) favors higher energy particles more strongly than ionization energy loss mechanisms]. As a result of these two balancing differences, about the same result is obtained.

Kellog argues that neutron decay is not an important source of electrons in the radiation belts. His argument, however, is based in large measure on electron flux measurements, which have, since then, been revised downward by as much as a factor of 10^3 . O'Brien, Van Allen, et al. (Reference 19) have recently determined that there were $\approx 10^8$ electrons/cm²-sec of energy greater than 40 kev in the outer belt on September 5, 1961. This was their highest reported flux; a time average of their values

might be several times lower than this figure. The observed flux at these energies is about a factor of 10 larger than our calculated value. Since exospheric densities are quite uncertain and acceleration processes may substantially increase the lifetime of the neutron-decay electrons, it is not at all compelling that sources other than neutron decay are required.

Lenchek, Singer, and Wentworth (Reference 15) have recently calculated the equilibrium flux of outer-belt electrons to be expected from neutron β decay in a manner somewhat like ours here. They consider Coulomb scattering and ionization energy loss of the electrons. The shape of the energy spectra they calculate agrees quite well with ours, but they arrive at different conclusions about the origin of the electrons observed in the radiation belt. They conclude that less than 5 percent of the electrons seen by Holly and Johnson (Reference 20) in the inner radiation belt at ≈ 1100 -km altitude are due to neutrons and that even a smaller fraction of the electrons seen by Cladis, Chase, et al. (Reference 21) at ≈ 1000 km in the outer belt are due to neutron decay. Lenchek and Singer state that neutron albedo contributes most if not all of the electrons above 400 keV but that few of the electrons of lower energy are made by neutrons.

We feel it is dangerous to base a general conclusion about the origin of all particles in the radiation belt on a few measurements at quite low altitudes. The analysis of these measurements depends on detailed information about the magnetic field of the earth's surface, the mirror-point altitude as a function of longitude, and the details of the atmosphere in a region where it is changing rapidly.

CONCLUSIONS

In this paper we have calculated the energy spectrum of electrons to be found in the outer belt if it were made of neutron β -decay electrons. Several experiments have given some information about the outer-belt spectrum, but the problem is not yet solved. The experiments involving bremsstrahlung will not be considered here because their interpretation is so difficult.

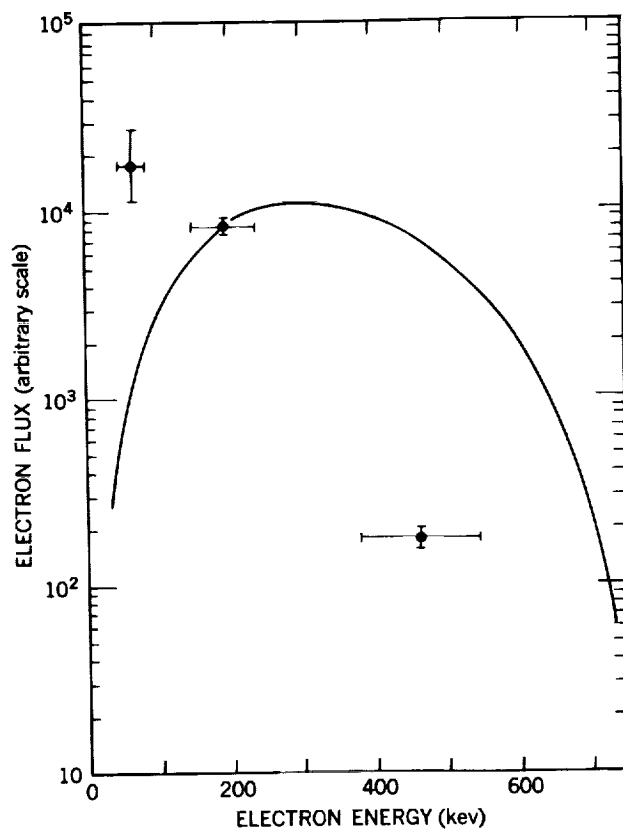


Figure 6—Electron-leakage flux spectrum. This curve shows, as a function of energy, the sum of all particles that are lost from the upper Van Allen radiation belt by multiple-Coulomb scattering, weighted by their lifetime at lower altitudes and multiplied by their velocity to yield a flux. The curve has been drawn arbitrarily to pass through the second experimental point of Cladis, Chase, et al. (Reference 21).

The Mechta experiment (References 22 and 23) indicated that there were about 1 percent as many electrons with $E > 500$ kev as with $E > 50$ kev. Our calculated spectrum gives about 8 percent for the ratio of particles with $E > 500$ to those with $E > 50$ kev. Experimentally, there may be fewer electrons in the few-hundred-kev range than we calculated, but this is quite sensitive to the energy-threshold setting. If the Mechta experiment threshold had actually been 600 kev instead of 500 kev, we would agree with the 1 percent figure.

The leakage-electron energy spectrum measured by Cladis, Chase, et al. (Reference 21) is steeper and shows more low-energy electrons than can be explained by neutron decay. The fact that measurement was carried out at quite low altitudes may mean that processes or electron sources are involved here that do not contribute at high altitudes.

O'Brien, Van Allen, et al. (Reference 19) have recently reported on the results of their experiment on Explorer XII (1961 v 1). They have measured the electron spectrum in the middle of the outer belt by using several detectors sensitive in different energy ranges. The spectrum devised from these measurements for September 5, 1961, is shown on Figure 7. Essentially, no electrons with $E > 5$ Mev were seen, but some electrons in the range $1.6 < E < 5$ Mev were probably observed, although the interpretation of these experimental results is not unique. These high-energy electrons are very important

for two reasons: First, they help explain results from several previous experiments that had seemed incompatible and, second, they cannot be made directly by neutron decay. There are not very many of these 1.6- to 5-Mev electrons; there were less than 1 percent of the total of September 5, and even less on other days.

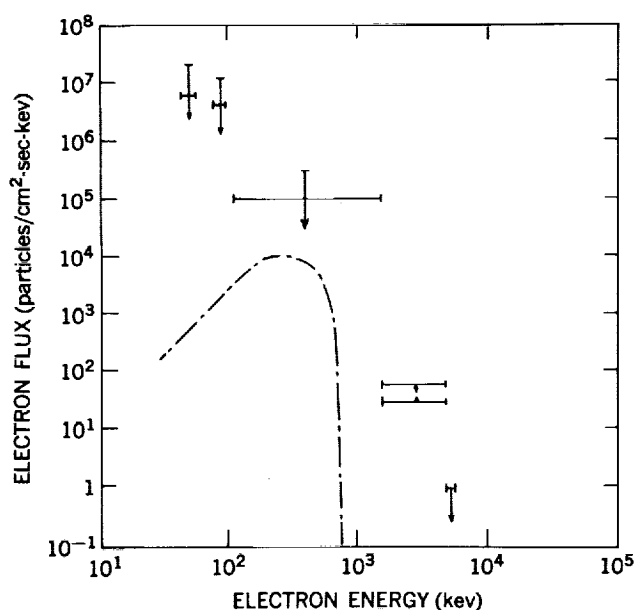


Figure 7—Equilibrium flux of electrons attained by trapping 3×10^{-13} electron/cm³-sec in an atmosphere of hydrogen of average density 10^{-21} gm/cm³. The incident spectrum is assumed to be that of a neutron-decay electron; the hydrogen is assumed to be about 50 percent ionized. The experimental points and limits are those of O'Brien, Van Allen, et al. (Reference 19) for September 5, 1961, when the electron flux was higher than average.

We must decide how similar the neutron β -decay electron energy spectrum is to the observed electron spectrum. Two features are to be compared: the shape, and the height—which amounts to comparing the flux. From Figure 7, in comparing the *shape* of the two spectra (aside from the electrons above 1.6 Mev) it is not obvious whether the spectral shapes agree or not. There may be too many low-energy electrons observed to agree with the calculated spectrum. One thing is certain: There is not the very large low-energy peak that earlier measurements indicated.

In comparing the *height* of the spectra we probably should not take the experimental spectrum in Figure 7 since it was the highest observed flux. We should decrease this by a factor

of 3 or more. Using a representative time-average flux of $\approx 3 \times 10^7$ electrons/cm²-sec for $E > 40$ kev (Reference 19), we find that our values are low by about one order of magnitude.

In this paper we have considered only neutrons made by galactic cosmic-ray protons. It is now quite certain that polar-cap protons contribute substantially to the low-energy trapped-proton spectrum (References 24, 25, and 26) by generating neutrons in the polar atmosphere. Polar-cap protons will also, in the same way, add considerably to the trapped-electron flux. Lenchek (Reference 27) has recently estimated that 100 times as many neutrons are generated by polar-cap protons as by galactic cosmic-ray protons. If our calculated electron flux were increased by a factor of 100, the calculated flux would exceed the measured flux.

It appears from this that neutron decays produce a reasonable fraction of the outer-belt electrons, but other processes such as acceleration may be important. Electrons above 1 Mev may be neutron β -decay electrons accelerated to these energies. We still need more definitive experiments to answer the question about whether any electron sources other than neutrons are needed to explain, in detail, the characteristics of the outer belt.

ACKNOWLEDGMENTS

We would like to thank Mrs. Kathryn Oliver, of the Lawrence Radiation Laboratory, for her assistance with the numerical calculations, and Professor Burton J. Moyer, University of California, for his support of this work. This work was done under the auspices of the U. S. Atomic Energy Commission.

REFERENCES

1. Freden, S. C., and White, R. S., "Particle Fluxes in the Inner Radiation Belt," *J. Geophys. Res.* 65(5):1377-1383, May 1960.
2. Hess, W. N., "Van Allen Belt Protons from Cosmic-Ray Neutron Leakage," *Phys. Rev. Letters* 3(1):11-13, July 1, 1959.
3. Hess, W. N., "The Radiation Belt Produced by Neutrons Leaking Out of the Atmosphere of the Earth," *J. Geophys. Res.* 65(10):3107-3115, October 1960.
4. Hess, W. N., Canfield, E. H., and Lingenfelter, R. E., "Cosmic-Ray Neutron Demography," *J. Geophys. Res.* 66(3):665-677, March 1961.
5. Christofilos, N. C., "Trapping and Lifetime of Charged Particles in the Geomagnetic Field," Univ. Calif., Radiation Lab. Rept. UCRL-5407, November 28, 1958.
6. Welch, J. A., Jr., and Whitaker, W. A., "Theory of Geomagnetically Trapped Electrons from an Artificial Source," *J. Geophys. Res.* 64(8):909-922, August 1959.

7. Wentworth, R. C., MacDonald, W. M., and Singer, S. F., "Lifetimes of Trapped Radiation Belt Particles Determined by Coulomb Scattering," *Phys. Fluids* 2(5):499-509, September-October 1959.
8. Nelms, A. T., "Energy Loss and Range of Electrons and Positrons," Washington: U. S. Government Printing Office, 1956 (U. S. Nat. Bur. Standards Circular 577).
9. Bethe, H. A., and Ashkin, J., "Passage of Radiations Through Matter," in: *Experimental Nuclear Physics*, ed. by E. Segrè, New York: John Wiley and Sons, 1953, Vol. 1, pp. 166-357.
10. "Symposium on Scientific Effects of Artificially Introduced Radiations at High Altitudes," *J. Geophys. Res.* 64(8):865-938, August 1959; also *Proc. Nat. Acad. Sci.* 45(8):1141-1228, August 15, 1959.
11. Møller, Chr., "Zur Theorie des Durchgangs Schneller Elektronen durch Materie," *Annalen der Physik* 14(5):531-585, August 15, 1932; see also Jauch, J. M., and Rohrlich, F., "The Theory of Photons and Electrons," Reading, Mass.: Addison-Wesley, 1955.
12. Bethe, H., "Quantenmechanik der Ein- und Zwei-Elektronenprobleme," in: *Handbuch der Physik*, ed. by H. Geiger and K. Scheel, Berlin: Springer-Verlag, 1933, Vol. 24, Pt. 1, pp. 273-560.
13. Christofilos, N. C., "The Argus Experiment," *J. Geophys. Res.* 64(8):869-875, August 1959.
14. Johnson, F. S., "The Exosphere and Upper F Region," *J. Geophys. Res.* 65(9):2571-2575, September 1960.
15. Lenchek, A. M., Singer, S. F., and Wentworth, R. C., "Geomagnetically Trapped Electrons from Cosmic Ray Albedo Neutrons," *J. Geophys. Res.* 66(12):4027-4046, December 1961.
16. Spitzer, L., Jr., "Physics of Fully Ionized Gases," New York: Interscience, 1956.
17. Arnoldy, R. L., Hoffman, R. A., and Winckler, J. R., "Observations of the Van Allen Radiation Regions During August and September 1959, Part 1," *J. Geophys. Res.* 65(5):1361-1376, May 1960.
18. Kellogg, P. J., "Electrons of the Van Allen Radiation," *J. Geophys. Res.* 65(9):2705-2713, September 1960.
19. O'Brien, B. J., Van Allen, J. A., et al., "Absolute Electron Intensities in the Heart of the Earth's Outer Radiation Zone," *J. Geophys. Res.* 67(1):397-403, January 1962; also State Univ. Iowa Rept. SUI 61-23, 1961.
20. Holly, F. E., and Johnson, R. G., "Measurement of Radiation in the Lower Van Allen Belt," *J. Geophys. Res.* 65(2):771-772, February 1960.
21. Cladis, A. B., Chase, L. F., Jr., et al., "Energy Spectrum and Angular Distributions of Electrons Trapped in the Geomagnetic Field," *J. Geophys. Res.* 66(8):2297-2312, August 1961.
22. Vernov, S. N., Chudakov, A. E., et al., "The Study of the Terrestrial Corpuscular Radiation and Cosmic Rays During the Flight of a Cosmic Rocket," *Soviet Phys.-Doklady* 4(2):338-342, October 1959.
23. Vernov, S. N., Chudakov, A. E., et al., "Radiation Measurements During the Flight of the Second Moon Rocket," *Soviet Phys.-Doklady* 5(1):95-99, July-August, 1960.

24. Armstrong, A. H., Harrison, F. B., et al., "Charged Particles in the Inner Van Allen Radiation Belt," *J. Geophys. Res.* 66(2):351-357, February 1961.
25. Naugle, J. E., and Kniffen, D. A., "Flux and Energy Spectra of the Protons in the Inner Van Allen Belt," *Phys. Rev. Letters* 7(1):3-6, July 1, 1961.
26. Naugle, J. E., and Kniffen, D. A., "The Flux and Energy Spectra of the Protons in the Inner Van Allen Belt," in: *Proc. Internat. Conf. on Cosmic Rays and the Earth Storm, Kyoto, September 1961. II. Joint Sessions*, Tokyo: Physical Society of Japan, 1962, pp. 118-122.
27. Lenchek, A. M., "On the Anomalous Component of Low-Energy Geomagnetically Trapped Protons," *J. Geophys. Res.* 67(6):2145-2157, June 1962.

